Available *online* at : http://jnte.ft.unand.ac.id/

Jurnal Nasional Teknik Elektro

| ISSN (Print) 2302-2949 | ISSN (Online) 2407-7267 |

Optimizing Lightning Arrester Selection for 275kV EHV Substations: A Comparison of Overvoltage Analysis with Software and Manual Calculations

Bagus Irawan Saputra [1], Marsul Siregar [2], Lanny W. Panjaitan [3]

[1] *Electrical Engineering Department, Universitas Katolik Indonesia Atma Jaya, Jakarta, 12930, Indonesia*

ARTICLE INFORMATION

Received: September 22. 2024
Revised: April 5, 2025
Accepted: June 20, 2025
Available online: July 31, 2025

KEYWORDS

CORRESPONDENCE

E-mail:bagusirawansaputra@gmail.com

A B S T R A C T

A substation is one of the essential aspects of an electrically interconnected system, especially in a grid utility. Power generation, transmission, and distribution systems always need a continuous power supply to the customer. In high voltage and extra high voltage substation, operation schemes during abnormal and normal conditions may cause transient overvoltage in the system, one of which is temporary overvoltage. Temporary overvoltage analysis is needed to validate the rated system voltage within the limit of the substation equipment's insulation level, including the rating of the lightning arrester. This research will select a lightning arrester with the standard approach IEC 60099-5 and software simulation on a computer. Conducted temporary overvoltage analysis using software simulation, which resulted in a value of 2.02 pu higher than the operating voltage. This slightly differs from the IEC 60099-5 standard, which recommends a value of 1.6 pu of operating voltage. Software simulation is beneficial as it models the system according to specific network parameters, leading to an optimal selection when compared to standards with different approaches to results based on varying network parameters. Temporary overvoltage analysis could help determine the correct rating of the lightning arrester and further mitigation, such as line compensation, switching technique, and load management, ultimately leading to reliability in substation equipment and interconnection system networks.

INTRODUCTION

In an electrical system, specifically in an interconnected electrical system, an HV/EHV substation is a major component [1]. It is one of the major electrical equipment in the transmission and distribution system [2]. Based on the utilization, the substation is used for voltage step-up or step-down. Due to the importance of the substation, the selection of equipment needs to be proper during the engineering design [1][3][4]. One of the parameters during design is temporary overvoltage [5].

TOV is a transient phenomenon that occurs when there is a sudden change in the load or fault condition in the power system[5] [6]. It is a general issue in power system networks, especially in high voltage (HV) and extra high voltage (EHV) networks.[2] [7]. It can lead to significant problems for the system's safe and reliable operation[8][6]. Temporary overvoltage is a type of overvoltage that can occur in a power system during the Ferranti effect, fault isolation, and load rejection events [9] [10] [4] [7]. IEC C62.82.1-2010 defines the temporary overvoltage as relatively happening in a long duration (seconds, even minutes) [11] [12] [13]. During these events, the voltage level in the system can increase to levels higher than the standard operating voltage[12] .

When overvoltage (TOV) occurs, the voltage level in the substation can exceed its standard operating range[9] [10]. This event is common in electrical network operation, and all equipment installed in the substation shall withstand overvoltage[14]. It will be different when the overvoltage happens in case of the switching transient (SFO), lightning (FFO), and transient enclosure voltage (VFFO), which can cause insulation breakdown, equipment damage, and voltage instability[2] [15] [16].

In the Croatian power network, Electra Zagreb, a temporary overvoltage of 2.3 per unit (pu) phase-to-earth was recorded. This overvoltage was amplified by network resonance, exceeding the standard equipment's withstand capabilities[9]. In Spanish, it is reported that transactions cause damage to metering and customer equipment, and also damage due to load rejection, causing temporary overvoltage[12]. Based on both cases, it is crucial to select the equipment rating and lightning arrester to withstand temporary overvoltage[17]. Additionally, identifying the factors that may cause or amplify temporary overvoltages is essential.

This paper will assess temporary overvoltage to validate the proper selection of the general voltage level requirement in the special TOV rating in the EHV substation[11] [16]. It may have a significant impact on substation operation in terms of a safe and reliable system in the power system network[18] [1] [19].

https://doi.org/10.25077/jnte.v14n2.1246.2025

Therefore, it is also essential to select the approach value of withstand voltage during the event of TOV to ensure the equipment is not damaged during regular operation[14]. On the other hand, lightning arrester can also be assessed to get proper value in terms of selection and sizing[11] [17] [1] [20].

METHODS

Temporary overvoltage (TOV) happening in a power system is complex. It depends on various factors such as the system topology, the characteristics of the power system components, and the system's transient response.

In general, TOV can occur due to a sudden change in the power system's voltage, current, or impedance. This can happen in various scenarios, including Ferranti effect load rejection and short circuit. Wrong selection of rating that may lead to its insulation breakdown, equipment damage, and voltage instability in the lightning arrester itself.

The risen voltage under the temporary overvoltage condition is divided into TOV limits 1s and 10s. This means that the lightning arrester will not operate if it is under its voltage and period limits. The lightning arrester cannot discharge the rising voltage due to temporary overvoltage, which is normal.

Interconnected System Model

The system model covered the transmission system of South Sulawesi. The specific location of this model is in the 275kV Pamona substation (275kV substation), as shown in the single-line diagram in Figure 1. This substation connects five main areas: South Sulawesi, Southeast Sulawesi, Middle Sulawesi, Poso-1 (Power Plant – 1), and Poso-2 (Power Plant – 2). Each feeder has 2 points of disconnector switches for bus transfer in case only one bus is available due to maintenance or a fault. The detailed configuration of the modelling equipment has been removed from this paper for confidential reasons.

The feeders are connected to the 275kV substation via short, medium, and long transmission lines. Power plants 1 and 2 supply around 300 MVA, associated with a short transmission line and modelled as an ideal source. South grid is supplied around 100MVA, connected with a long transmission line, and simply with the grid model (interconnected system of the south grid). The Southeast Sulawesi grid is supplied around 30MVA, connected with a medium transmission line, and simply with a lump load model. The Middle Sulawesi grid is supplied around 100MVA, connected with a medium transmission line, and connected to the grid model(interconnected system of the middle grid).

A lightning arrester is not modelled in the system model because the lightning arrester will operate in switching transient, lightning transient, and very fast transient overvoltage. Temporary overvoltage is a normal operating condition that allows overvoltage to happen in the system.

Feranti Effect

The Ferranti effect is a phenomenon that can cause temporary overvoltage in long transmission lines due to the resonance of the line capacitance and inductance. It occurs when a long transmission line is lightly loaded or unloaded, causing the line capacitance to affect the line impedance significantly. Typically, the duration of the Ferranti effect ranges from seconds to minutes. As the voltage in the line increases, the capacitance of the line also increases, leading to an increase in reactive power flow. This increase in reactive power flow causes the voltage in the line to increase further, leading to TOV.

Short Circuit (SLG)

When a short circuit occurs, the voltage level in the system can increase due to the flow of ground fault current. The short circuit duration in an interconnected system is typically less than 1 second. This current can cause a voltage drop across the system's impedance, increasing voltage in other parts. During an SLG fault, one phase of a three-phase power system comes into contact with the ground, creating a low-impedance path for current flow.

Load Rejection

The increase in voltage during load rejection can occur due to the inductive nature of the power system. Typically, the duration of load rejection in an interconnected system is less than 1 second. When the load is suddenly disconnected, the system’s inductance causes the current to flow briefly. This current can cause a voltage drop across the system's impedance, increasing voltage in other parts.

Fault Isolation

Similarly, fault and load rejection events can cause TOV. Typically, the fault isolation duration in an interconnected system is less than 1 second. The fault isolation event combines clearing the fault and a load rejection event. The IEC standard does not mention a simultaneous combination of fault isolation and load rejection. This case mostly happens when a fault in the transmission line may lead to overvoltage.

TOV Parameter for Lightning Arrester Selection based on IEC 60099-5

This section performs the standard sizing and calculation for lightning arresters based on IEC 60099-5. The steps are defined as follows:

https://doi.org/10.25077/jnte.v14n2.1246.2025

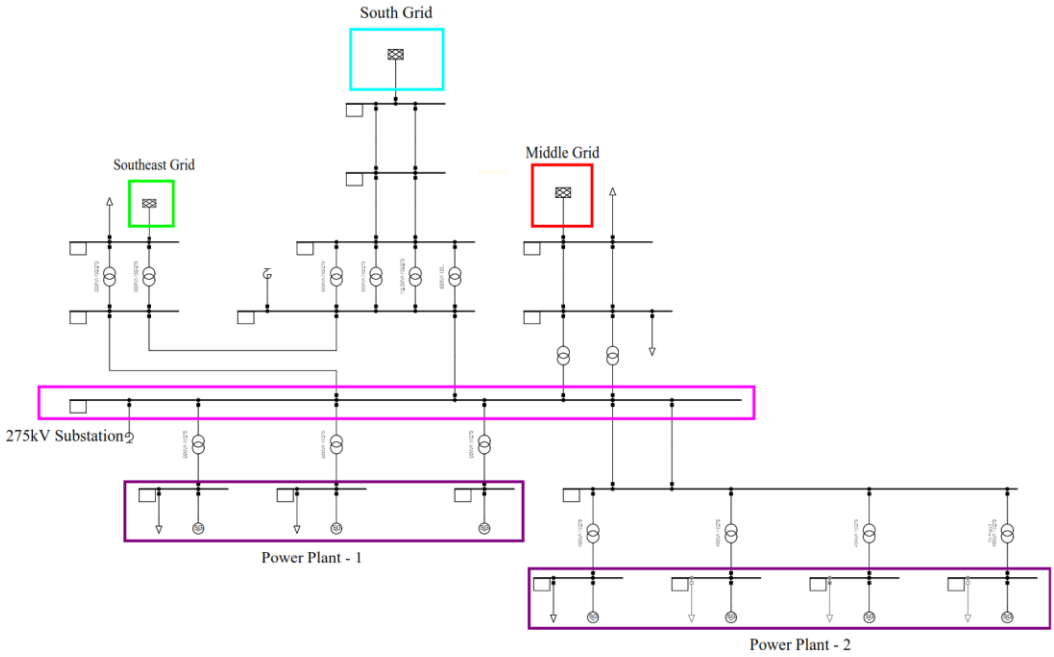

Figure 1. Overall Single Line Diagram

Step 1: Determine voltage classification, such as standard operating voltage (Un) and rated voltage (Us)
Step 2: Determine the UC (continuous operation voltage)

$$\text{Uc} = \frac{1{,}05 \text{ x Us}}{\sqrt{3}}$$

Step 3: Determine the Ur (rated voltage operation voltage)

$$\text{Ur} = \frac{Uc}{0{,}8}$$

Step 4: Determine the typical overvoltage based on SLG, Load Rejection, and Ferranti Effect
Step 5: Select the lightning arrester based on the manufacturer's datasheet.

TOV Parameter Selection Based on Software Simulation

In this section, the lightning arresters will be selected by modeling the network based on the given data and defining cases caused by the Ferranti effect, single ground fault, load rejection, and fault isolation. The PSCAD software, which features EMT study capabilities, will simulate all the cases. The steps are defined as follows:

Step 1: Create an interconnected system model and determine the system
Step 2: Calculate the source impedance, determine the line, load, and bus parameters.
Step 3: Create a case study, such as the Ferranti effect, SLG fault, load rejection, and fault isolation.
Step 4: Determine the selection of multiple runs of the simulation based on timing and fault sequence (SLG, load rejection, and fault isolation) to achieve peak value
Step 5: Select the lightning arrester based on the manufacturer's datasheet.

System Model Parameter

The system model for TOV simulation mainly consists of the source, tower geometry, load, and bus parameters. The source model can be determined by given parameters such as voltage (L-L) and (L-N), frequency, 3-phase short circuit, and 1-phase source circuit, and X/R (3-Phase) and X/R (1-Phase). It is necessary to calculate the source impedance to be input as source parameters. The steps for source model calculations are determined below:

Step 1: Determine the data from the grid utility as the basis of the source impedance calculation.
$U_{(L-L)}, U_{(L-N)}, C_{factor}, I_{sc\,(3-phase)}, I_{sc\,(1-phase)}$, and X/R
Step 2: Determine the Positive Sequence

$$Z_{1.2} = \frac{C_{factor} \text{ x } U_{(L-L)}}{\sqrt[2]{3} \text{ x } I_{sc\,(3-phase)}} \quad (1)$$

$$X_{1.2} = \frac{Z_1}{\sqrt[2]{1 + (R_1/X_1)^2}} \quad (2)$$

$$R_{1.2} = \frac{X_{1.2}}{Z_{1.2}} \quad (3)$$

Step 3: Determine the Zero Sequence

$$Z_0 = \frac{3U_{(L-N)}}{(I_{sc\,(1-phase)} - 2 \text{ x } Z_1} \quad (4)$$

$$R_0 = \frac{Z_0}{\sqrt{1+(X/R)^2}} \quad (5)$$

$$X_0 = \sqrt{Z_0^2 - R_0^2} \quad (6)$$

Step 4: Performing a validation model to ensure that the rms value during the short circuit simulation will be the same as the given data of the 3-phase short circuit and the 1-phase source circuit.

The tower geometry can be defined based on the provided parameters, considering the type of conductor and the arrangement of the towers. The software will automatically calculate the positive, negative, and zero sequence impedance using the Geometric Mean Distance (GMD) and Geometric Mean Radius (GMR) methods. Load analysis can be performed based on the specified data parameters, such as the ZIP load model, and the bus configuration can be determined according to the type of substation typically used in a double busbar system.

Simulation Methods

The simulation method will use multiple runs, in which the simulation will be repeated for each case and each combination

case. Multiple run is a feature of the software that continuously determines the maximum and minimum values of repeated simulations, finding the maximum value to determine the maximum TOV, as input lightning arrester selection is essential.

RESULTS AND DISCUSSION

System Parameter

$U_n = 275\ kV_{rms}$
$U_{s\ or\ m} = 300\ kV_{rms}$

Lightning Arrester Manufacturer Datasheet

Table 1. Manufacturer Datasheet ABB EXLIM Q-D

Max	Rated Voltage	Max. Continuous Operating Voltage 1)		TOV Capability 2)	
		As per IEC	As per ANSI/IEEE		
Um	Ur	Uc	MCOV kVrms	1s	10s
300	216	173	175	250	237
	228	182	182	264	250
	240	191	191	278	264
	258	191	209	299	283
	264	191	212	306	290

Table 1 is the baseline for determining the arrester rating using manual calculations and simulation approaches.

Selection Based on IEC 60099-5 2018

Lightning Arrester Sizing

Step 1: Calculate Uc
$\text{Uc} = \frac{1{,}05\ \text{x Us}}{\sqrt{3}} = \frac{1{,}05\ \text{x 300kV}}{\sqrt{3}} = 181{,}865 kV\text{rms}$

Step 2: Calculate Ur
$\text{Ur} = \frac{Uc}{0{,}8} = \frac{181{,}865\ kV}{0{,}8} = 227{,}331 kV\text{rms}$

Step 3: Determine typical temporary overvoltage
$1\ \text{p.u} = \frac{Us\ x\ \sqrt{2}}{\sqrt{3}} = \frac{300kV\ x\ \sqrt{2}}{\sqrt{3}} = 257{,}196\ kV_{peak}$
$U_{SLG} = 1.3 \sim 1{,}4\ \text{p.u} = 334{,}355 \sim 360{,}075\ kV_{peak}$
$U_{LR} = 1.2 \sim 1{,}5\ \text{p.u} = 308{,}635 \sim 385{,}794\ kV_{peak}$
$U_{FE} = 1.02\ \text{p.u} = 262{,}340\ kV_{peak}$

Step 4: The rating is changed into the RMS value
$U_{SLG} = 236{,}424 \sim 253{,}611\ kV_{rms}$
$U_{LR} = 218{,}238 \sim 272{,}798\ kV_{rms}$
$U_{FE} = 185{,}502\ kV_{rms}$

Step 5: Lightning Arrester Selection
Based on rating steps 1 to 4, the selection of lightning arrester ratings is:
$U_{s\ or\ m} = 300\ kV_{rms}$: based on the system rating voltage
$U_r = 240\ kV_{rms}$: same or greater than calculation
$U_c = 191\ kV_{rms}$: same or greater than calculation
$TOV_{1s} = 278 kV_{rms}$: the highest value of load rejection or SLG
$TOV_{10s} = 264\ kV_{rms}$: highest value Ferranti effect

Table 2. Arrester Selection Based on Manual Calculation

Max	Rated Voltage	Max. Continuous Operating Voltage 1)		TOV Capability 2)	
		As per IEC	As per ANSI/IEEE		
Um	Ur	Uc	MCOV kVrms	1s	10s
300	240	191	191	278	264

Table 2 presents the results of selecting the lightning arrester based on manual calculations, utilizing IEEE6099-5:2018 and considering typical outcomes per the standard.

Note :
Uc : Continuous operating voltage
Ur : Rated system voltage
U_{SLG} : Overvoltage during SLG in the healthy phase
U_{LR} : Overvoltage during load rejection
U_{FE} : Overvoltage during the Ferranti effect
TOV_{1s} : Ability to withstand TOV for 1s
TOV_{10s} : Ability to withstand TOV for 10s

Selection Based on Simulation

Source Model

The source model was modelled using data provided by the grid utility company. To model the source as a voltage source, it is necessary to calculate the positive/negative and zero sequence resistance and reactance of the interconnected system of the south and middle grid. The value will be used as given below :

Interconnected Supply South Grid Data:
$U_{(L-L)} = 150kV \quad U_{(L-N)} = 86{,}6kV$
$f = 50\ Hz$
$C_{factor} = 1.05$
$I_{sc\ (3-phase)} = 3{,}849\ kA$
$I_{sc\ (1-phase)} = 4{,}075\ kA$
$X_{1.2}/R_{1.2} = 25$ and $X_0/R_0 = 25$

Positive/Negative Sequence Calculation :
Step 1: Define the $Z_{1.2}$
$Z_{1.2} = \frac{C_{factor}\ x\ U_{(L-L)}}{\sqrt[2]{3}\ x\ I_{sc\ (3-phase)}} = 23{,}62501102$
Step 2: Define the $X_{1.2}$
$X_{1.2}/R_{1.2} = 25$; $X_{1.2} = 25R_{1.2}$
$X_{1.2} = \frac{Z_1}{\sqrt[2]{1 + (R_1/X_1)^2}}$
$\sqrt[2]{1 + (R_{1.2}/X_{1.2})^2} = \sqrt[2]{1 + (1/25)^2} = 1{,}0008$
$X_{1.2} = \frac{23{,}62501102}{1{,}0008} = 23{,}60613366\ ohm$
Step 3: Define $R_{1.2}$
$R_{1.2} = \frac{X_{1.2}}{25} = \frac{23{,}60613366}{25} = 0{,}944245346\ ohm$
Step 4: Source Model Validation

https://doi.org/10.25077/jnte.v14n2.1246.2025

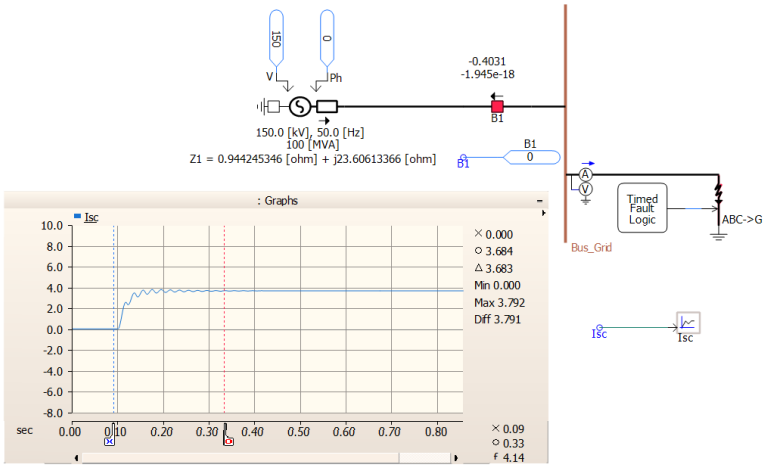

Figure 2. Short Circuit 3-Phase

The model was validated based on Figure 2 by providing a 3-phase short circuit, which resulted in 3,792 kA. This result is the same as the input data, which is 3,849 kA.

Zero Sequence Calculation :

Step 1: Determine the Z_0

$$I_{sc\,(1-phase)} = \frac{3\ x\ U_{(L-N)}\ x\ C_{factor}}{(Z_1 + Z_2 + Z_0)}$$

$$Z_0 = (\frac{3\ x\ U_{(L-N)}\ x\ C_{factor}}{I_{sc\,(1-phase)}}) - (Z_1 + Z_2) = 19{,}7320277$$

X_0/R_0 =25 ; $X_0 = 25R_0$

$$Z_0 = \sqrt[2]{(R_0)^2 + (X_0)^2} = \sqrt[2]{(R_0)^2 + (25R_0)^2} = 25{,}01999201$$

Step 2: Define R_0

$$R_0 = (\frac{Z_0}{\sqrt[2]{1 + (X_0/R_0)^2}}) = 0{,}78865044\ ohm$$

Step 3: Define the X_0

$X_0 = 25R_0 = 19{,}716261$ ohm

Step 4: Source Model Validation

The model was validated based on Figure 3 by providing a 1-phase to ground short circuit, which resulted in 2,302 kA ($I_{(L-g)}$). The line-to-line value is 2.343 kA x $\sqrt[2]{3}$ *which is* 4.058 kA ($I_{(L-L)}$).. This result is similar to the input data, which is 4,075 kA.

The rest of the middle grid and power plant source model used the same calculations. The model was implemented and integrated before conducting the simulation.

Feranti Effect

Case 1, shown in Figure 4, was simulated under normal conditions. The reactor in the 275kV south grid substation was disconnected. The reactive power is produced in the 208 km 275kV south grid substation. The voltage peak phase to ground occurs at 252,568 kVpeak.

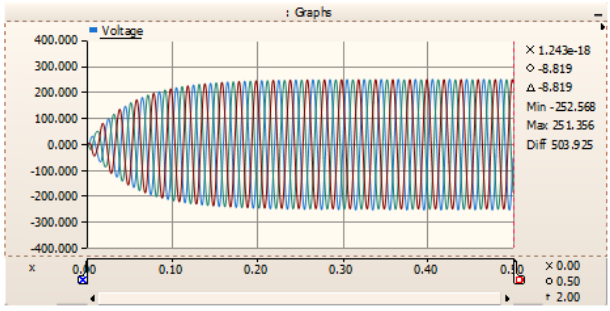

Figure 3. Vpeak at 275kV substation without reactor connected

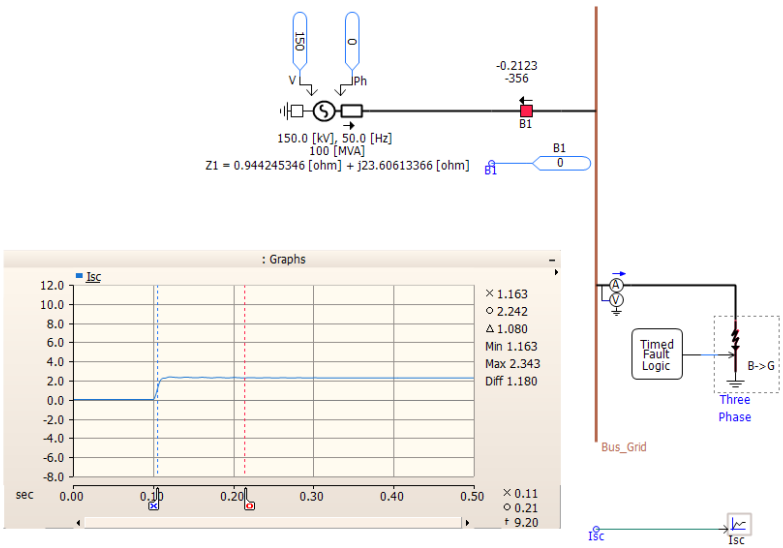

Figure 4. Short Circuit 1-phase to ground

Case 2, shown in Figure 5, was simulated under normal conditions. The reactor in the 275kV south grid substation was connected to compensate for the reactive power produced from the 208 km 275kV south grid substation—the reactor model was an MVAr load for each line, 50MVA. The voltage peak phase to ground occurs at 219.702 kVpeak.

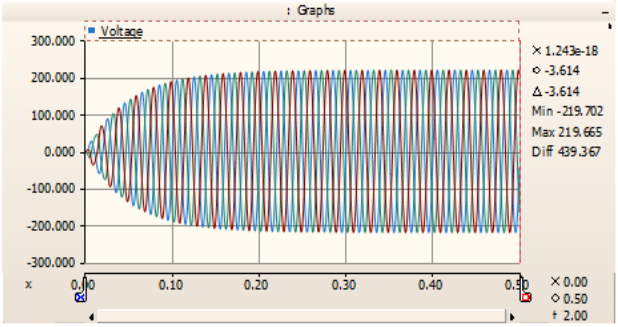

Figure 5. Vpeak at 275kV substation with reactor connected

Figure 4 shows overvoltage results from stray capacitance in the transmission line, especially in long transmission lines. This condition occurs during transmission line energization and grid start-up. The stray capacitance will produce reactive power over the transmission line and cause overvoltage due to the Ferranti effect. The optimum model uses distributed parameters to determine the tower and conductor impedance value. Stray capacitance will produce distributed reactive power over the transmission line due to the inductance and resistance.

Figure 5 shows an overvoltage damped by the reactor in the 275kV south grid substation. The reactor absorbs the reactive power from a long transmission line. The voltage is decreased because the line reactor absorbed the stray capacitance.

Short Circuit (SLG)

Case 1, as illustrated in Figure 6, simulates a single-line-to-ground (SLG) fault condition occurring at the 275 kV substation. The simulation was performed using eleven time steps ranging from 0.30 seconds to 0.40 seconds, with 10-millisecond increments, to observe the time-dependent behavior of transient overvoltages. This setup aims to evaluate the severity and variation of peak overvoltages under different fault inception times within the same fault location.

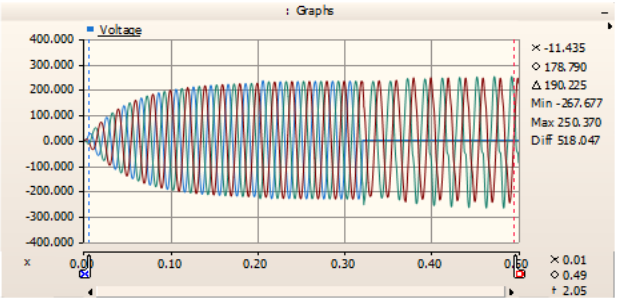

Figure 6. SLG Fault – 275kV Substation

Figure 6 illustrates the SLG fault condition located at the 275 kV substation. The fault is applied to a single-phase conductor, while the other phases remain healthy during the event. This configuration allows the study of overvoltage phenomena on the non-faulted phases and helps understand insulation stress in the event of ground faults within a high-voltage substation.

The results of the simulation are summarized in Table 3, which presents the peak line-to-ground (L-G) overvoltage observed for each time step of fault initiation. The peak overvoltage recorded in this case reaches 267.68 kV at 0.32 seconds, indicating a moment of maximum transient stress. From Table, it is evident that although the overvoltage values vary slightly across the tested time range, they generally remain within a high voltage range above 250 kV, which could pose risks to equipment if not properly insulated.

Table 3 Voltage Result

No	Fault Sequence	Peak Overvoltage (L-G)
1	0.30 s	267.6668109
2	0.31 s	263.9302743
3	**0.32 s**	**267.6767159**
4	0.33 s	261.6457908
5	0.34 s	267.2578379
6	0.35 s	259.4686670
7	0.36 s	265.5607452
8	0.37 s	259.4023211
9	0.38 s	262.4391382
10	0.39 s	257.9396294
11	0.40 s	257.6177948

Case 2, depicted in Figure 7, involves an SLG fault introduced at a different location — the South Grid Substation — which is approximately 208 kilometers away from the 275 kV substation. This case uses the same fault initiation pattern as Case 1, with eleven simulation steps from 0.30 to 0.40 seconds at 10-millisecond intervals. The objective of this scenario is to observe the effect of fault distance on the resulting transient voltages experienced at the receiving end.

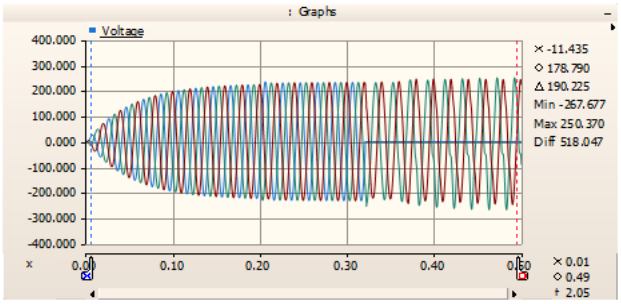

Figure 7. SLG Fault – 275kV Substation

Figure 7 shows the simulated fault at the South Grid Substation, which represents a remote fault scenario compared to the main 275 kV station. The introduction of the fault at a distant location allows analysis of the voltage profile over a long transmission line. The results help evaluate the damping effect of line impedance and the reduction of transient severity with increasing fault distance.

The simulation output is shown in Table 4, where peak line-to-ground overvoltages are listed for each fault inception time. The recorded overvoltage values in this scenario are relatively consistent, with the highest reaching 244.85 kV at 0.40 seconds. Compared to Case 1, these values are significantly lower,

https://doi.org/10.25077/jnte.v14n2.1246.2025

suggesting that distance plays an important role in reducing transient overvoltages at the main substation during SLG conditions occurring farther away.

Table 4 Voltage Result

No	Fault Sequence	Peak Overvoltage (L-G)
1	0.30 s	244.3459201
2	0.31 s	244.3321174
3	0.32 s	244.5392172
4	0.33 s	244.4903551
5	0.34 s	244.6683219
6	0.35 s	244.5964853
7	0.36 s	244.7543977
8	0.37 s	244.6676875
9	0.38 s	244.8116376
10	0.39 s	244.7154783
11	**0.40 s**	**244.8495572**

Load Rejection

Case 1, shown in Figure 8, was simulated with load rejection incoming at the 275kV south grid substation and the 275kV southeast grid substation in the 275kV substation. The simulation will be done based on 11 times multiple sequence starts from 0.3s to 0.4s with a grading of 10ms.

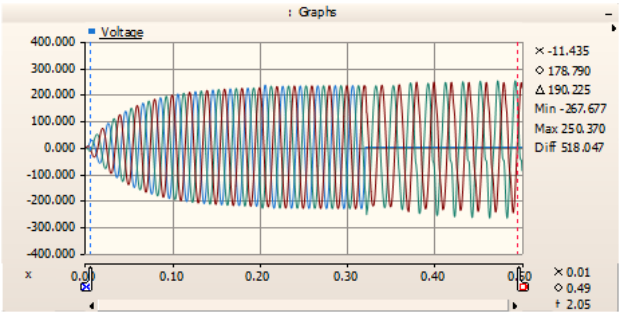

Figure 8 Load Rejection – Incoming Line South Grid and Southeast Grid 275kV Substation.

Table 5 Voltage Result

No	Opening Sequence	Peak Overvoltage (L-G)
1	0.30 s	239.8488988
2	0.31 s	239.8551030
3	0.32 s	239.8482909
4	0.33 s	239.8544479
5	0.34 s	239.8947133
6	0.35 s	239.8537661
7	0.36 s	239.9524702
8	0.37 s	239.8883055
9	0.38 s	239.9909312
10	0.39 s	239.9221270
11	**0.40 s**	**240.0164481**

Figure 8 and Table 5 describe overvoltage during load rejection in the 275kV substation. The peak voltage occurs at 0.40s with 240,016 kVpeak.

Case 2, shown in Figure 9, was simulated by load rejection of 2 outgoing 275kV south grid substations and 275kV southeast grid substation in each substation. The simulation will be done based on 11 times multiple sequence starts from 0.3s to 0.4s with a grading of 10ms.

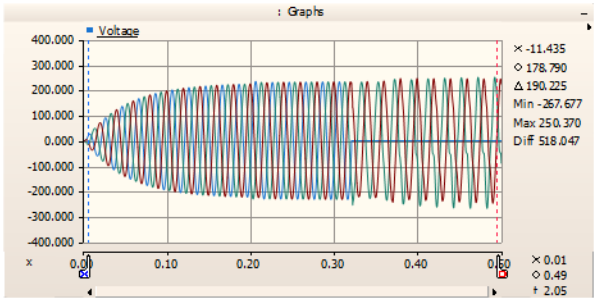

Figure 9. Load Rejection – Incoming Line South Grid and Southeast Grid 275kV Substation.

Table 6 Voltage Result

No	Opening Sequence	Peak Overvoltage (L-G)
1	0.30 s	332.3016581
2	0.31 s	326.4186228
3	0.32 s	332.4665813
4	0.33 s	326.4549060
5	0.34 s	332.5508186
6	0.35 s	326.4435814
7	**0.36 s**	**332.5817358**
8	0.37 s	326.4003476
9	0.38 s	332.5770340
10	0.39 s	326.3365114
11	0.40 s	332.5502236

Figure 9 and Table 6 describe the overvoltage during a single-line to ground fault in a 275kV substation. The peak voltage occurs at 0.36s with 332,581 kV.

Fault Isolation

The simulation will consider performing fault clearing and load rejection with the assumption of 100ms after the fault happens. The simulation will take 2 cases:

Case 1, as shown in Figure 10, the simulation will perform fault clearing and load rejection on the outgoing line to the south grid and the southeast grid Substation in each substation. The simulation will be done based on 11 times multiple sequence starts from 0.3s to 0.4s with a grading of 10ms for fault. The load rejection will be done based on an 11 times multiple sequence, starting from 0.4s to 0.5s with a grading of 10ms. The total simulation is 121 cases based on a combination of fault and load rejection, but we select only the clearing time with a total below 100ms, which produces 65 instances.

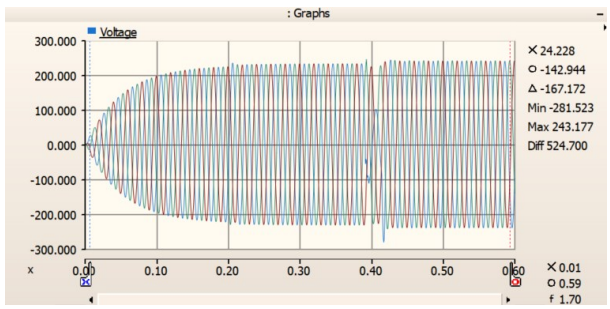

Figure 10. Fault + Load Rejection – Outgoing Line South Grid and Southeast Grid Substation

Table 7 Voltage Result

No	Fault Sequence	Opening Time	Peak Overvoltage (L-G)
1	0.39 s	0.41 s	281.523

Figure 10 and Table. 7 Describe the overvoltage during a single-line to ground fault in a 275kV substation. The peak voltage occurs at 0.41s with 281,552kVpeak.

Case 2, as shown in Figure 11, the simulation will perform fault clearing and load rejection on the incoming line 275kV south grid substation and 275kV southeast grid substation at the 275kV substation. The simulation will be done based on 11 times multiple sequence starts from 0.3s to 0.4s with a grading of 10ms for fault. The load rejection will be done based on an 11 times multiple sequence, starting from 0.4s to 0.5s with a grading of 10ms. The total simulation is 121 cases based on a combination of fault and load rejection, but we select only the clearing time with a total below 100ms, which produces 65 instances.

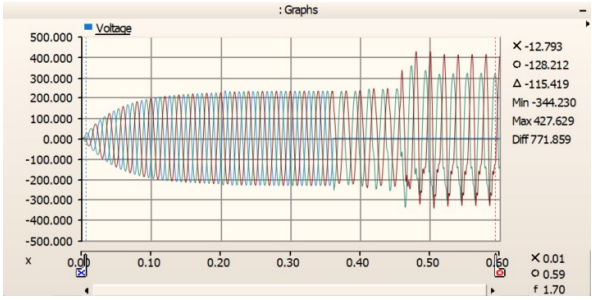

Figure 11. Load Rejection – Incoming Line South Grid and Southeast Grid 275kV Substation.

Table 8 Voltage Result

No	Fault Sequence	Opening Time	Peak Overvoltage (L-G)
1	0.36 s	0.45 s	427.629

Figure 11 and Table 8 describe the overvoltage during a single-line to ground fault in the 275kV substation. The peak voltage occurs at 0.45s with 427,629 kVpeak.

Simulation Result

The simulation results for the Ferranti effect, single-line-to-ground (SLG) faults, load rejection, and fault isolation are shown in Tables 9 and 10. These tables compare how transient overvoltages respond to different disturbances, highlighting peak voltage (Vp), RMS voltage (Vrms), fault timing, and opening times for each case.

Table 9 Voltage Summary Based on Ferranti and SLG

No	Description	Feranti Effect		Single Line to Ground Fault	
		#1	#2	#1	#2
1	Vp	252,568 kV	219.702 kV	267.676 kV	244.849 kV
2	Vrms	178,592 kV	155,352 kV	181,497 kV	173,134
3	Fault Sequence			0.32 s	0.40 s
4	Opening Time				

Table 9 presents a voltage summary comparing the Ferranti effect and SLG fault scenarios. In Case 1 of the Ferranti condition, the peak voltage reaches 252.568 kV, while the RMS voltage is 178.592 kV, representing the highest continuous operating voltage observed under this effect. In contrast, the SLG fault in Case 1 results in a higher peak voltage of 267.676 kV, occurring at 0.32 seconds, while Case 2 records a slightly lower peak of 244.849 kV, occurring at 0.40 seconds. The variation in fault sequence times indicates the dynamic nature of overvoltage propagation depending on fault location and system conditions.

Table 10 Voltage Summary Based on Load Rejection and Fault Isolation

No	Description	Load Rejection		Load Rejection during clearing Single Line to Ground Fault	
		#1	#2	#1	#2
1	Vp	240.016 kV	332,581 kV	281,523kV	427,629 kV
2	Vrms	169,716 kV	235,125 kV	199,066kV	**302,379 kV**
3	Fault Sequence	-	-	0.39 s	0.36 s
4	Opening Time	0.40 s	0.36 s	0.41 s	0.45 s

Table 10 highlights the voltage behavior under load rejection and fault isolation events. In the case of load rejection alone (Cases #1 and #2), the peak voltages recorded are 240.016 kV and 332.581 kV, respectively, with RMS voltages reaching 235.125 kV in Case 2. When load rejection occurs during SLG fault clearance, more significant overvoltage is observed. In Case 2 of fault isolation, the peak voltage reaches 427.629 kV at 0.45 seconds, making it the highest instantaneous overvoltage recorded across all scenarios. The corresponding RMS voltage for this event is 302.379 kV, confirming that fault isolation with delayed opening can lead to critical transient stress on system insulation.

Overall, the simulation demonstrates that fault isolation, particularly with delayed breaker operation, can result in significantly higher overvoltage conditions compared to other events such as Ferranti effects or SLG faults alone. These findings highlight the importance of timely fault clearing and optimized opening times to mitigate transient voltage spikes.

Lightning Arrester Selection

$U_{s\,or\,m} = 300\ kV_{rms}$
$U_r = 268\ kV_{rms}$
$U_c = 191\ kV_{rms}$
$U_{LR} = 235{,}557$
$TOV_{1s} = 306\ kV_{rms}$
$TOV_{10s} = 290\ kV_{rms}$

Based on the simulation rating of Uc, or maximum continuous overvoltage, the Ferranti effect is defined as the worst case. The reactor was open, and the long transmission line produced reactive power to the grid. The value shall be equal to or greater than 178,592 kVrms, suitable for 191kVrms (see Table 7).

https://doi.org/10.25077/jnte.v14n2.1246.2025

The simulation result of the highest possibility of overvoltage from the three simulations, except for the Ferranti effect, is fault isolation. It is selected as the rating of TOV1's capability, and its value shall be the same or greater than 302,379kVrms, which is suitable with 306kVrms (see Table 8).

Table 11. Arrester Selection Based on Simulation

Max	Rated Voltage	Max. Continuous Operating Voltage 1)		TOV Capability 2)	
		As per IEC	As per ANSI/IEEE		
Um	Ur	Uc	MCOV	1s	10s
			kVrms		
300	264	191	212	306	290

Taking into account the findings presented in Tables 9 and 10, the selection of the lightning arrester is made according to Table 11

Discussion

The simulation model approach and sequencing events provide more accurate results than manual calculations. As noted by H. Ghoddami & A. Yazdani, A. Abdullah & B. Yancey, and Gefei Kou, determining temporary overvoltages involves assessing the sequence of events, several scenarios, and loading conditions, which aids in identifying the most critical cases. Similarly, this research adopts the same methodology.[2], [3]

The potential to amplify voltage during a temporary overvoltage (TOV) event may originate from capacitors, high impedance, or ungrounded networks. Based on A. Aaron Kalyuzhny's findings show that TOV results can potentially exceed permissible limits in the presence of resonance grounding. Therefore, numerical simulations shall be conducted to analyze and obtain accurate results. Similarly, this research combines conventional approaches with software simulations to enhance the analysis. [9]

On the other hand, the B. Rittong and S. Sirisumrannukul research suggests reducing voltage by increasing the neutral earthing resistor. However, this approach leads to an increase in TOV levels. They recommend replacing existing lightning arresters with higher-rated ones to address the TOV issue. Similarly, this research emphasizes selecting the highest-rated lightning arresters by assessing the maximum possible overvoltage caused by temporary overvoltage.[5]

Based on Table 12 below, the result of manual calculations compared with the simulation result is slightly different in $TOV_{(1s)}$.

Table 12 Manual and Software Calculation

No	Description	Result	
		Manual Calculation	Simulation Result
1	Uc	181,865 kVrms	178,592 kVrms
2	TOV(1s)	294,447 kVrms	302,379 kVrms
3	TOV(10s)	185,502 kVrms	178,592 kVrms

To address the lightning arrester selection, the Uc/MCOV and $TOV_{(1s)}$. It is mandatory to select the highest value to avoid the voltage clipping/discharge during normal conditions.

Table 13 Lightning Arrester Selection

No	Description	Result	
		Manual Calculation	Simulation Result
1	Uc	191 kVrms	191 kVrms
2	TOV(1s)	278 kVrms	306 kVrms
3	TOV(10s)	264 kVrms	290 kVrms

Table 13 shows that the selection of a lightning arrester shall consider the highest overvoltage possibility, which is obtained by using simulation results to give a more precise value.

CONCLUSIONS

In this research, the selection of arresters can be performed both manually and through simulation. The manual calculation considers standardized overvoltage possibilities based on typical values and information from numerous publications regarding related overvoltage phenomena, as summarized in IEC 60099-5. However, to optimize the insulation level of the equipment, further analytical modeling and simulation of power system transients are necessary. Additionally, more studies may be required to evaluate the response of lightning arresters during events of slow front overvoltage (SFO), fast front overvoltage (FFO), and very fast front overvoltage (VFFO). The assessment related to insulation coordination encompasses several key aspects: SFO pertains to the energization and re-energization of equipment, such as transformers and line shunt reactors; FFO is associated with direct lightning strikes and back-flashover events; and VFFO applies specifically to gas-insulated substations (GIS) during the switching of the GIS isolator. Conducting these studies will provide a comprehensive understanding of high-voltage substation design that goes beyond merely considering lightning arresters.

REFERENCES

[1] R. M. Arias Velásquez and J. V. Mejía Lara, "The problem of the actual insulation coordination for 500 kV with overvoltage in substations and the needed for more surge arresters in high voltage grid," *Ain Shams Eng. J.*, vol. 14, no. 9, p. 102130, Sep. 2023, doi: 10.1016/j.asej.2023.102130.

[2] H. Ghoddami and A. Yazdani, "A Mitigation Strategy for Temporary Overvoltages Caused by Grid-Connected Photovoltaic Systems," *IEEE Trans. Energy Convers.*, vol. 30, no. 2, pp. 413–420, Jun. 2015, doi: 10.1109/TEC.2014.2364033.

[3] A. Abdullah and B. Yancey, "A Reduced Order Model for a TOV Study in a Solar PV Project," in *2017 IEEE 44th Photovoltaic Specialist Conference (PVSC)*, Washington, DC: IEEE, Jun. 2017, pp. 2128–2134. doi: 10.1109/PVSC.2017.8521539.

[4] A. Cerretti, F. M. Gatta, A. Geri, S. Lauria, M. Maccioni, and G. Valtorta, "Temporary overvoltages due to ground faults in MV networks," in *2009 IEEE Bucharest PowerTech*, Bucharest, Romania: IEEE, Jun. 2009, pp. 1–8. doi: 10.1109/PTC.2009.5282140.

[5] B. Rittong and S. Sirisumrannukul, "Assessment of Voltage Sag and Temporary Overvoltage for Neutral Grounding Resistance in Distribution System," in *2019 IEEE PES GTD Grand International Conference and Exposition Asia (GTD Asia)*, Bangkok, Thailand: IEEE, Mar. 2019, pp. 796–801. doi: 10.1109/GTDAsia.2019.8715885.

[6] H. Saad and S. Dennetiere, "Study on TOV after Fault Recovery in VSC based HVDC systems," in *2019 IEEE Milan PowerTech*, Milan, Italy: IEEE, Jun. 2019, pp. 1–6. doi: 10.1109/PTC.2019.8810479.

[7] I. Sadeghkhani, A. Ketabi, and R. Feuillet, "Estimation of Temporary Overvoltages during Power System Restoration using Artificial Neural Network," in *2009 15th International Conference on Intelligent System Applications to Power Systems*, Curitiba: IEEE, Nov. 2009, pp. 1–6. doi: 10.1109/ISAP.2009.5352836.

[8] S. Carsimamovic, Z. Bajramovic, O. Hadzic, and A. Carsimamovic, "Modeling and Calculation of Switching Overvoltages in 400 kV Electrical Networks," in *EUROCON 2005 - The International Conference on "Computer as a Tool,"* Belgrade, Serbia and Montenegro: IEEE, 2005, pp. 1521–1524. doi: 10.1109/EURCON.2005.1630254.

[9] A. Kalyuzhny, "Analysis of Temporary Overvoltages During Open-Phase Faults in Distribution Networks With Resonant Grounding," *IEEE Trans. Power Deliv.*, vol. 30, no. 1, pp. 420–427, Feb. 2015, doi: 10.1109/TPWRD.2014.2327074.

[10] D. Yang, Z. Xiang, R. Song, L. Shen, P. Zhou, and Y. Yang, "Research on Temporary Overvoltage in PMSG-based Wind Power Transmission System in case of Load Rejection," in *2020 5th Asia Conference on Power and Electrical Engineering (ACPEE)*, Chengdu, China: IEEE, Jun. 2020, pp. 469–474. doi: 10.1109/ACPEE48638.2020.9136353.

[11] A. Chennamadhavuni, K. Kumar Munji, and R. Bhimasingu, "Investigation of transient and temporary overvoltages in a wind farm," in *2012 IEEE International Conference on Power System Technology (POWERCON)*, Auckland, New Zealand: IEEE, Oct. 2012, pp. 1–6. doi: 10.1109/PowerCon.2012.6401440.

[12] G. Kou *et al.*, "Load Rejection Overvoltage of Utility-Scale Distributed Solar Generation," *IEEE Trans. Power Deliv.*, vol. 35, no. 4, pp. 2113–2116, Aug. 2020, doi: 10.1109/TPWRD.2019.2951949.

[13] T. Sakurai, K. Murotani, and K. Oonishi, "Suppression of Temporary Overvoltages Caused by Transformer and AC Filter Inrush Currents at the Shin-Shinano Frequency Converter Station," *IEEE Trans. Power Appar. Syst.*, vol. PAS-100, no. 4, pp. 1608–1613, Apr. 1981, doi: 10.1109/TPAS.1981.316549.

[14] T. T. Quoc, S. L. Du, D. P. Van, N. N. Khac, and L. T. Dinh, "Temporary overvoltages in the Vietnam 500 kV transmission line," in *ESMO '98 - 1998 IEEE 8th International Conference on Transmission and Distribution Construction, Operation and Live-Line Maintenance Proceedings ESMO '98 Proceedings. ESMO 98 The Power is in Your Hands*, Orlando, FL, USA: IEEE, 1996, pp. 225–230. doi: 10.1109/TDCLLM.1998.668378.

[15] R. A. Walling, "Overvoltage protection and arrester selection for large wind plants," in *2008 IEEE/PES Transmission and Distribution Conference and Exposition*, Chicago, IL, USA: IEEE, Apr. 2008, pp. 1–5. doi: 10.1109/TDC.2008.4517283.

[16] C. Lothongkam, T. Patcharoen, and S. Yoomak, "Effect of the drop out fuse connection scheme on the overvoltage and the surge arrester in a distribution system," *Energy Rep.*, vol. 9, pp. 41–47, Oct. 2023, doi: 10.1016/j.egyr.2023.08.058.

[17] M. V. Lat, "Determining temporary overvoltage levels for application of metal oxide surge arresters on multigrounded distribution systems," *IEEE Trans. Power Deliv.*, vol. 5, no. 2, pp. 936–946, Apr. 1990, doi: 10.1109/61.53105.

[18] X. Liu, H. Xin, D. Zheng, and B. Cao, "Temporary overvoltage assessment and suppression in heterogeneous renewable energy power systems," *Int. J. Electr. Power Energy Syst.*, vol. 155, p. 109472, Jan. 2024, doi: 10.1016/j.ijepes.2023.109472.

[19] M. Yoon, X. Zhang, and S. Choi, "Strategic intentional islanding method considering temporary overvoltage in disaster situations," *Int. J. Electr. Power Energy Syst.*, vol. 165, p. 110488, Apr. 2025, doi: 10.1016/j.ijepes.2025.110488.

[20] R. M. Arias Velásquez, "Transient analysis of temporary overvoltage and cable faults in underground medium voltage systems," *Results Eng.*, vol. 25, p. 103875, Mar. 2025, doi: 10.1016/j.rineng.2024.103875.

AUTHOR(S) BIOGRAPHY

Bagus Irawan Saputra hold a master's degree from Electrical Engineering Department of Atma Jaya Catholic University of Indonesia. He received his bachelor's degree in electrical engineering from Universitas Hasanuddin, Makassar, in 2018. He is an electrical engineer working in a private engineering company and developing an electrical community called teknikelektroid and ASTDK, which focuses on power system study. His research interests lie in high voltage and power system studies.

Marsul Siregar Marsul Siregar was born in Medan, North Sumatera, on August 5, 1960. He received a B.Eng degree from the Department of Electrical Engineering, Faculty of Engineering, North Sumatera University, Medan in 1986. He completed the Master's Engineering Degree and Doctors Engineering Degree in Tokushima University Japan, on 1993 and 1996. His research interest is Renewable Energy and Power Systems. Now He is lecturer in Electrical Engineering Department of Atma Jaya Catholic University of Indonesia.

Lanny W. Panjaitan was born in Kudus, on February 2, 1947. She received his B.Eng degree from Bandung Institute of Technology, Bandung-West Java, in 1973. He completed the Master's Engineering degree and Doctors Engineering degree from Bandung Institute of Technology in Bandung-West Java, on 1994 and 2000, respectively. Her research interests is Electronic, Artificial Intelligece, and Intelligent Control and System. Now she is a professor in Electrical Engineering Department of Atma Jaya Catholic University of Indonesia.

https://doi.org/10.25077/jnte.v14n2.1246.2025